Adipose Tissue Derived Mesenchymal Stem Cells (ADMSCs) Protect Against Hyperglycemia and Hyperlipidemia Induced Heart Failure by Inhibiting Autophagy Related Apoptosis

Xu Xu
Shanghai Tenth People's Hospital https://orcid.org/0000-0002-9019-8449
Sujing Qiang
Shanghai Tenth People's Hospital
Lingyun Tao
Shanghai Laboratory Animal Research Center
Jie Zhou
Shanghai Laboratory Animal Research Center
Jing Ni (15900750278@163.com)
Shanghai Tenth People's Hospital https://orcid.org/0000-0002-0297-471X

Research Article

Keywords: heart failure, hyperglycemia, hyperlipidemia ADMSCs, IL-1β, autophagy

Posted Date: June 22nd, 2021

DOI: https://doi.org/10.21203/rs.3.rs-606381/v1

Abstract

Background

Mesenchymal stem cells (MSCs), kinds of seed cells, are expected to improve impaired diabetic cardiac function. Inflammation and autophagy play the important role in the development of metabolic disorder induced heart failure. The aim of this work was to assess the effect of adipose tissue derived mesenchymal stem cells (ADMSCs) on metabolic disorder induced heart failure and the underlying mechanisms.

Methods

In vivo, 8 weeks old male C57BL/6 mice were randomly divided into three groups: normal chaw mice (sham group), high fat diet fed and streptozotocin intraperitoneal injected mice (HFD + STZ group) and ADMSCs tail intravenous injected per week for 3 months after the mice were treated with HFD + STZ (ADMSCs + HFD + STZ group). The lipid and glucose levels as well as echocardiography were measured per week. Immunohistochemistry was used to detect the adhesion of macrophages in heart tissue among three groups. Besides, inflammatory cytokines such as interleukin-1β (IL-1β), tumor necrosis factor α (TNFα), interleukin-6 (IL-6) and interleukin-8(CXCL-15) were measured by western blot or RT-qPCR. In vitro, H9c2 cardiomyocytes were stimulated to 33mM glucose in the presence or absence of IL-1β. Transmission electron microscope, mRFG-GFP-LC3 assay and flow cytometry were used to investigate autophagy related apoptosis in H9c2 cells.

Results

HFD + STZ treated mice presented significant cardiac hypertrophy, body weight loss, hyperglycemia and hyperlipidemia. However, these changes were remarkably reversed by ADMSCs administration. The administration of ADMSCs also remit histological alterations and deposition of collagen in the heart tissue. Furthermore, ADMSCs downregulated the adhesion of macrophages in heart tissue. More importantly, IL-1β from macrophages increased the autophagy of myocardial cell stimulated with high glucose which eventually leaded to their apoptosis and the following cardiac dysfunction.

Conclusions

This study confirmed that ADMSCs may have potential for use in improving cardiac function by restraining autophagy and apoptosis of myocardial cell. We also found the roles of the IL-1β in hyperglycemia and hyperlipidemia induced cardiac injuries, which may be a key factor for diabetic complications.

Introduction

Previously, Framing Ham study have indicated that patients with diabetes mellitus (DM) have 2 times higher risk in men and 5 times higher risk in women to have heart failure (HF) than the age matched controls[1]. Other clinical studies also have proved that patients with. And most of them have LV diastolic dysfunction rather than LV systolic dysfunction in both T1DM and T2DM patients[3] and animal models[4]. These eventually leaded to the occurrence of some asymptomatic heart disease in diabetic populations. However, a recent study from Mayo clinic based on a larger patient population hold a different opinion. They have demonstrated slightly lower LVEF in diabetic patients compared to normal people. More importantly, patients with decreased LVEF would have worse survival even in diabetic asymptomatic heart disease[5]. Thus, it is needed to investigate the possible strategy to improve cardiac function of patients with DM.

It has been widely recognized that hyperglycemia and hyperlipidemia might be the main metabolic reasons for the clinical progression of cardiovascular diseases (CVD), including heart failure[6]. Hyperlipidemia is also considered as a major risk factor for CVD in type II diabetes mellitus[7, 8].The animal model also indicated that blood lipid lowering could inhibit pressure overloaded (transverse aortic constriction)[9] or myocardial infarction induced heart failure[10] by promoting Ca2 + induced permeability transition in mitochondria. Here, we construct an animal model to investigate the role of hyperglycemia and hyperlipidemia induced HF with reduced left ventricular ejection fraction (HFrEF).

Mesenchymal stem cells (MSCs) are the most common cells which have been applicated for cardiac diseases[11, 12]. Recent works have found that MSCs could enhance cardiac function and reduce the size of myocardial infarction properly by interfering with autophagy flow in the animal model[13, 14]. There are different kinds of MSCs, including bone marrow-derived mesenchymal stem cells (BMSCs) and adipose tissue-derived mesenchymal stem cells (ADMSCs). The content of ADMSCs is approximately 1:1500 and is more than BMSCs[15]. ADMSCs can be acquired conveniently and have multi-lineage capacity, which differentiate into adipose, bone, cartilage, cardiac muscle and epithelial cell types[16, 17]. ADMSCs are capable of inhibiting oxidative stress and inflammation by different mechanisms in experimental diabetic models[9, 18]. Previous studies have showed that ADMSCs decreased the expression of pro-inflammatory cytokines such as TNF-α and IL-6, ameliorated the systematic inflammation in septic rats[19]. According to Sun M et al, ADMSCs could decrease STAT3 and STAT6 expression and exert anti-inflammatory role due to their effect on Mφ to M2b/c-Mφ[9]. Thus, it is reasonable to hypothesize that ADMSCs could be used to protect the cardiac function of hyperglycemia and hyperlipidemia induced HFrEF as well.

Methods

Ethics Statement

All animal experimental procedures were carried out in accordance with the guidelines of the Shanghai Experimental Animal Center and the Shanghai Tenth People's Hospital (SYXK: 2014-0026) “People and Animal Use in Research” and in accordance with the principles set out in the Helsinki Declaration. Experimental animals are treated humanely, and all efforts are made to alleviate their discomfort. All mice were housed in a specific pathogen-free animal vivarium and maintained on a 12h light, 12h dark cycle, with free access to standard rodent chow and water.

Isolation and Culture of ADMSCs

SD rats were purchased from Shanghai Research Center of the Southern model organisms (China). ADSCs were isolated from the subcutaneous adipose tissue of 8 to 12-week-old SD rats. Briefly, The adipose tissue was obtained from the subcutaneous fat pad around the ilium of the rats and was washed in phosphate-buffered saline (PBS) (CORNING, Manassas, USA) containing 1% Penicillin-Streptomycin□PS□solution (HyClone, Pasching, Austria). We minced the fat pad into pieces and then lysised them in Dulbecco's modified Eagle's medium (DMEM) (Thermo Fisher, Suzhou, China) containing 1 mg/ml collagenase I (YEASEN, Shanghai, China) and 1% PS at 37°C for 30 min. The digested tissue was filtered through a sterile 100 μm nylon mesh (Corning, NY, USA), and centrifuged at 1800 rpm for 5 min. After that, we discarded the supernatant and resuspended the pellet with culture medium twice. ADSCs were seeded onto culture dishes with growth medium DME/F-12 (HyClone, GE Healthcare Life Sciences, Logan, Utah, USA) containing 10% fetal bovine serum (FBS) (Sigma-Aldrich) and 1% PS at 37°C in a humidified atmosphere of 5% CO_2 before being using for analysis.

Animal Study

8-weeks-old male C57BL/6 mice were purchased from Shanghai Research Center of the Southern model organisms (China). Type I diabetes was induced with the dose of streptozotocin (STZ, 70mg/kg in 0.1mol/L citrate buffer solution; Sigma-aldrich, St. Louis, Missouri, USA) intraperitoneally injected per two days. 8 weeks later, the blood glucose level (fasting blood glucose over 16.6mmol/L were considered as diabetic) were measured. The diabetic mice were tail vein injected with ADMSCs (2×10^6) or saline for 12 weeks. Body weight, random blood glucose levels and blood lipid level as well as echocardiography were tested at the time points. 30 weeks after the model establishment, all animals were sacrificed and heart tissues were isolated for further analysis.

Echocardiography

The echocardiography was performed by using a Vevo 2100 High Resolution Imaging System (Visual Sonics, Toronto, Canada). Briefly, mice were anesthetized by isoflurane (1%) and placed on the 37.C platform. Parasternal long axis (PSLAX) images were acquired and analyzed with a VevoStrain software. From the M-mode images, the diameter of the left ventricle (LV) at the end of the diastole (LVEDD) and systole (LVESD), LV fractional shortening (FS), and LV ejection fraction (EF) were calculated by the machine.

Cell culture and stimulation

H9c2 cardiomyocytes were purchased from the Institute of Biochemistry and Cell Biology (Shanghai, China). Cells were incubated in DMEM containing with 10% FBS and 1%PS. For high glucose administration, cells were incubated with culture media containing 33 mM glucose for 72 hours. H9c2 cardiomyocytes were treated with high glucose (HG, 33mM), IL-1β (20ng/ml, popertech, cat#400-01B), IL-1β and HG respectively after they were starved for 3 hours. And untreated cells were used as negative control.

Histopathology staining

Myocardial tissue was fixed with 4% paraformaldehyde and dehydrated and embedded in paraffin. Next, the samples were cut into 5-μm-thick sections that should be undertaken. Heart sections were stained with hematoxylin-eosin (H&E), Masson's trichrome and wheat germ agglutinin (WGA) staining. The muscle cells with clear nuclear nucleus and clear sarcolemma were selected for analysis of muscle cell cross-sectional area (CSA) in H&E staining and WGA staining. Fibrosis was detected on the heart tissue by Mason trichrome staining. 4 microscopic photographs of every section were shot randomly selected by NIS-elements v3.0 (Nikon, Japan). Cardiac CSA and myocardial fibrosis were analyzed Image-ProPlus6.0 software (Media Cybernetics, Silver Spring, Maryland, USA) for quantitative analysis. Date expressed as mean ± standard deviation.

Immunohistochemistry

The myocardial tissues were fixed in 4% paraformaldehyde and then embedded in paraffin after dehydration. Next, the samples were cut into 5-μm-thick sections. After that , the sections were deparaffinized and stained with F4/80（diluted concentration 1:200, Servicebio, Wuhan, China). For IHC analysis, each section was captured in at least 5 images by NIS-elements v3.0 (Nikon, Japan) and all images were quantified using Image-ProPlus6.0 software (Media Cybernetics, Silver Spring, Maryland, USA). Percentages of positive stains for F4/80 within the fields were averaged for each mouse and then for each group as described before. Date expressed as mean ± standard deviation.

Western blotting analysis

Total protein was extracted from mouse hearts and the levels were determined using a BCA Protein Assay Kit (Thermo Scientific, Rockford, Illinois, USA). Equal amounts of total protein (50 μg) were loaded and then separated by sodium dodecyl sulfate polyacrylamide gel electrophoresis (SDS-PAGE) and transferred to PVDF membranes (Thermo Scientific, Rockford, Illinois, USA). The membranes were then blocked in 5% BSA (YEASEN, Shanghai, China) for 1 h, followed by overnight incubation at 4 °C with the following primary antibodies: IL-1β (cat: mAb #12242, diluted concentration 1:1000, Cell Signaling Technology, Danvers, MA, USA), P62 (cat：ab109012, diluted concentration 1:800, abcam, England), LC3I/II (cat: ab62721, diluted concentration 1:500, abcam, England), DAPDH (cat: ABS16, diluted concentration 1:10000, EMD Millipore Corp, USA). The secondary antibodies were horseradish peroxidase

(HRP)-linked-Antibody, anti-rabbit IgG (diluted concentration 1:5000, Cell Signaling Technology, Danvers, MA, USA) and horseradish peroxidase (HRP)-labeled-Antibody, Goat Anti-Mouse IgG (diluted concentration 1:5000, Biosharp Life Sciences, Hefei, China). Blots were processed for enhanced chemifluorescence using a Pierce ECL western blotting substrate (Tanon, Shanghai, China). Images were collected using ChemiDoc™ MP Imaging System (Bio-Rad, Hercules, CA, USA). Bands on immunoblots were quantified by densitometry using Image Lab software (version 6.0, Bio-Rad).

Real-time quantitative polymerase chain reaction (RT-qPCR)

Total RNA was purified from mouse hearts with TRIZol ((Thermo Scientific, Rockford, Illinois, USA)) following manufacturer's protocol. The total RNA was used for reverse-transcription and amplified using a One Step SYBR RT-PCR Kit (TaKaRa, Shiga, Japan). After that, the cDNA was amplified with SYBR Premix Ex Taq (KAPA, Cape, South Africa) by a Real-Time PCR System (Roche, Basel, Swiss). GAPDH was used as the internal control. The sequences of the primers for each gene detected are listed in Supplementary Table 1. The PCR program was as follows:95℃,10 min; 95℃,5s60℃,34s for a total of 40cycles. The expression levels of target genes were determined using the 2−ΔΔCT method. Table 1. Primers

Annexin V-FITC/PI staining and flow cytometry

H9c2 cells were treated as described above and were stained by using FITC Annexin V/Dead Cell Apoptosis Kit (cat: v13242, Invitrogen,USA) according to the manufacturer's instructions. Then, cells were diluted in the dilution buffer and the apoptotic cells were measured by a BD FACS Calibur flow cytometer (BD Biosciences, Heidelberg, Germany) in a total of 10,000 counted cells.

Transmission electron microscope and observation of autophagosome

Briefly, the cell medium was removed. Then, cells were washed with 0.1 cacodylate buffer and fixed with a solution containing 3% glutaraldehyde and 2% paraformaldehyde in PBS. Later, the rest of the procedure was conducted using the standard protocol. Transmission electron microscope (JEM-1400PLUS) was used to obtain the images.

mRFG-GFP-LC3 assay

H9c2 cardiomyocytes were seeded into the six-well-plate to reach about 60% confluence. Later, they were divided into 4 groups (NC group, HG group, IL-1β group, HG+ IL-1β group) and transfected with adenovirus (20 MOI, HBAD-mRFP-GFP-LC3, Hanbio, Shanghai, China) for another 48 hours. In brief, cells were fixed in 4% paraformaldehyde for 10 mins and were washed by PBS for three times. The, they were sealed by 10% glycerinum to limit fluorescence quenching. Leica DMI6000 was used to detect related fluorescence. The GFP signals were observed in the lysosomal acidic conditions, whereas mRFP fluorescence was relatively stable. Therefore, this tandem-tagged fluorescent protein showed yellow dots in the autophagosomes, while exhibited red only in lysosomes. Quantification of GFP and mRFP

fluorescence dots, and overlay between two different signals were recorded and analyzed using ImageJ software.

Statistical analysis

All data are shown as the mean±SEM. Student's t-test (two-sided), one-way ANOVA or two-way ANOVA followed by Bonferroni's pos-hoc test were used to calculate *P* value accordingly. Error bars represented standard errors, and numbers of experiments (n) were as indicated. $P < 0.05$ was regarded as significant. All statistical analyses were performed using SPSS 20.0 software.

Results

Adipose tissue-derived mesenchymal stem cells(ADMSCs)improved glycometabolism and lipid metabolism of high-fat diet/STZ -induced diabetic mice.

In order to investigate the potential of adipose tissue-derived mesenchymal stem cells (ADMSCs) in mice with hyperglycemia and hyperlipidemia, three-month-old male C57BL/6 mice treated with STZ were feed either a high fat (HF) or normal chow (NC). Later, ADSCs were injected into the STZ + HF group mice by tail vein injection as described in method. After 8 weeks, STZ induced diabetic mice fed with HF diet exhibited a slightly decreased body weight compared with NC group mice. And the body weight barely changed in ADMSCs + HFD + STZ treated mice (Fig. 1A). Accordingly, the serum glucose level of HF + STZ treated mice was higher than NC group mice. And the treatment of ADMSCs could improve the glycometabolism of HFD + STZ treated mice as shown in Fig. 1B. These mice have an abnormal higher serum glucose level, but their serum glucose was reduced by the injection of ADMSCs. Besides, it could be noticed that the triglyceride of ADMSCs + HFD + STZ treated mice also decreased a lot. Nonetheless, the enhanced serum cholesterol, high-density lipoprotein and low-density lipoprotein in HFD + STZ group were unchanged after ADMSCs treatment (Fig. 1C-1F). In conclusion, ADMSCs injection could greatly ameliorate the hyperglycemia and hyperlipidemia in STZ induced diabetic mice in combination of HF diet.

Adipose tissue-derived mesenchymal stem cells(ADMSCs)alleviated heart failure of high-fat diet/STZ -induced diabetic mice.

To explore whether ADMSCs could alleviate heart failure in HFD + STZ induced mice with metabolic disorder or not, these mice were subjected to perform echocardiography to evaluate their cardiac function. Although the overlooks of the harvested hearts have no distinguished differences between groups, the ventricular wall thickness were increased in HFD + STZ group mice. The administration of ADMSCs restrict the hypertrophic ventricular wall thickness in HFD + STZ treated mice (Fig. 2A). The data obtained from echocardiography have verified a recovery of the cardiac function in ADMSCs injected HFD + STZ group mice as well (Fig. 2B). More preciously, the heart rates maintained in the same level with or without treatments (Fig. 2C). It could be observed that the HFD + STZ fed mice have a declined cardiac function with decreased ejection function (EF, Fig. 2D), left ventricular short-axis shortening rate

(FS, Fig. 2E) and an increased left ventricular internal dimension (LVID, Fig. 2F) compared to sham groups. After operation, the data from ADMSCs injected HFD + STZ group mice showed that ADMSCs could promote EF, FS and decrease LVID compared with mice without injection (Fig. 2D-2G). The HE staining of cardiac cross sections revealed that HF + STZ group mice have more vacuolization of cardiomyocytes. But the administration of ADMSCs eliminated these pathologic changes (Fig. 2H). Further, the pictures taken from masson stained cardiac cross sections proved that the deteriorated cardiac function could be attributed to the serious fibrosis of cardiac tissue in HFD + STZ mice. Meanwhile, the treatment of ADMCSs in HFD + STZ group mice greatly suppressed the fibration of heart tissue (Fig. 2J-2I). In line with these results, the WAG staining of demonstrated that ADMSCs might inhibit the enlargement of cardiomyocytes occurred in HFD + STZ fed mice. Taken together, our results have clarified that ADMSCs could cardiac dysfunctions of HFD + STZ fed mice.

Adipose tissue-derived mesenchymal stem cells(ADMSCs)suppressed adhesion of macrophages and the secretion of IL-1β in vitro and in vivo.

Recent researches have revealed that ADMSCs could suppress inflammation by regulating the polarization of macrophages and regulating the population of M1 and M2 macrophages[20, 21]. Also, macrophages have been indicated their roles in cardiac remodeling in HF and were considered as clinical target of HF [22, 23]. IF staining was done to figure out the effect of ADMSCs on macrophages and the procession of HF. It could be observed that the F4/80 positive cells in cardiac tissue of HFD + STZ induced diabetic mice were increased. And the treatment of ADMSCs markedly inhibited the adhesion of macrophages in HFD + STZ group mice (Fig. 3A-3B). Consistent with this result, the enhanced secretion of IL-1β was also decreased due to the limitation of macrophages in cardiac tissue with the help of ADMSCs (Fig. 3C-3D). Besides, the mRNA levels of other inflammatory cytokines such as tumor necrosis factor α (TNFα), interleukin-6 (IL-6), interleukin-8 (CXCL15) were also restrained by the administration of ADMSCs (Fig. 3E-3G). Above all, it is reasonable to suspect that ADMSCs dismissed the progression of heart failure by reducing inflammation and related cytokines such as IL-1β from macrophages.

IL-1β enhanced diabetic cardiomyopathy by inhibiting autophagy and increasing apoptosis in H9c2 cells.

IL-1β is a cytokine which has been identified its role in accelerating the progression of heart failure[24, 25]. Canakinumab, an IL-1β inhibitor, also has been applicated in clinical trial to prevent hospitalization for heart failure[25]. Yet, the mechanism of IL-1β to improve the occurrence of heart failure was still unascertained. The results have indicated ADMSCs could decrease the distribution of IL-1β in heart. HFD + STZ induced diabetic mice exhibited a severe fibration but a slight enlargement of myocardial hypertrophy in cardiac tissue. This phenomenon suggested the possibility of reduced number of cardiomyocytes in HFD + SZT group mice. H9c2 cells were stimulated with IL-1β and high glucouse at the same time for 72 hours. IL-1β + HG treated cells have a larger population of apoptosis in all cells than IL-1β or HG stimulated cells(Fig. 4A-4B). The images obtained from transmission electron microscope showed more autophagic vacuolization in IL-1β + HG stimulated group than other two groups (Fig. 4C). In addition, the immunoblot of p62 and LC3I/II were measured to monitor autophagic flux as well. Of course,

IL-1β + HG promoted the expression of LC3I/II and inhibited the expression of LC3 I/II and p62 which suggested the autophagy was enhanced in these cells. (Fig. 4D-4E). To confirm these results, tandem fluorescent mRFG-GFP-LC3 assay was performed to detect the autophagic flux. IL-1β + HG group cells have increased red foci which proved a weaker autophagic flux in the cells compared to other controls (Fig. 5A-5C). Thus, ADMSCs might prevent the diabetic cardiomyopathy by promoting autophagy and apoptosis in IL-1β + HG stimulated cells.

Discussion

Previously, it has been well known that ADMSCs can differentiate into adipose, bone, cartilage and epithelial cell types[13, 14]. Our data have proved that the injection of ADMSCs in HFD + STZ group mice greatly prevented the progression of HF compared to sham group mice. However, ADMSCs might not distributed into the heart directly which means that they might insert their function with the help of other cell types[26, 27]. The result was future confirmed by the higher positive F4/80 staining of macrophages in the ADMSCs treated group. Macrophages have been indicated their roles in HF especially in myocardial infarction (MI) induced HF[22]. They were main contributors to the inflammatory and fibrotic processes in HF. Moreover, DM and insulin resistance were also associated with progression of HF[28, 29]. Our data provided a clue that ADMSCs have the potential to attract macrophages into the heart tissue of hyperglycemia and hyperlipidemia induced HF. Also, macrophages have different subtype such as M1, M2, tumor associated macrophages (TAM), CD169macrophages and TCRmacrophages[30, 31]. The results from our researcher have verified that the increased macrophages in heart tissue of HFD + STZ group mice were properly M1 type macrophages. These macrophages could release some inflammatory cytokines such as IL-1β and TNFα. Nevertheless, precise classification should be performed by flow cytometric sorting as M1 type macrophages expressed CD14, CD11b, CD68 and MAC-1/MAC-3.

Also, it should be noted that the precious distribution of ADMSCs was not clear as they were not labeled to trace their confluence in particular organs. Earlier studies have demonstrated the distribution of ADMSCs was based on the type of injury[32, 33]. The majority of ADMSCs were attracted to damaged tissue and related region lack of blood and nutrition. Therefore, further experiments should be done to confirm how do they promote the adhesion of macrophages in the heart.

Besides, the enrichment of macrophages in the heart tissue of HFD + STZ group mice also increased the IL-1β. Myocardial cells exposed in the microenvironment of hyperglycemia and hyperlipidemia were lack of nutrition supply properly. They preferred to evoke autophagy pathway to save energy and keep themselves from apoptosis[1, 34]. Lee et al have verified ATG7(autophagy related gene) knockout mice could not survive over 12 hours because they showed their disability of nutrition supply[35]. Yet, there were a controversy about the role of inflammation on autophagy. Some researchers insisted that autophagy could accelerated inflammation[36, 37]. Other researcher held the opposite views that hyperglycemia and hyperlipidemia would decrease the inflammation and apoptosis of myocardial cells by promoting autophagy[38, 39]. In our study, we noticed that inflammatory cytokines such as IL-1β could activated

autophagy of H9c2 cells and increased degree of autophagy in co-existence with hyperglycemia. And the improvement eventually aggregated the apoptosis of H9c2 cells. In conclusion, our data supported the synergistic effect of IL-1β and hyperglycemia in autophagy. However, it was noted that our data only discussed the specific situation of inflammation which was focused on the increase of IL-1β. The diversity of inflammatory cytokines in inflammatory microenvironment made our discussions were limited on a scope. More research should be designed to further discus these problems.

Declarations

Funding

This study is supported by grants No. 91939104 from the Chinese National Natural Science Foundation.

Conflicts of interest

The authors declare that there is no conflict of interests regarding the publication of this article.

Availability of data and material and Code availability

All data and materials as well as software application or custom code support our published claims and comply with field standards.

Author Contribution

Xu xu and Sujing Qiang performed the animal experiments, cell function, and conducted western blot, immunofluorescence, and analyzed data. Lingyun Tao and JieZhou helped interpret the data and wrote the manuscript. Jing Ni conceived the project, designed experiments, analyzed data, interpreted results and wrote the manuscript.

Ethics approval

All animal experimental procedures were carried out in accordance with the guidelines of the Shanghai Experimental Animal Center and the Shanghai Tenth People's Hospital (SYXK: 2014-0026) “People and Animal Use in Research” and in accordance with the principles set out in the Helsinki Declaration. Experimental animals are treated humanely, and all efforts are made to alleviate their discomfort. All mice were housed in a specific pathogen-free animal vivarium and maintained on a 12h light, 12h dark cycle, with free access to standard rodent chow and water.

Consent to participate

Not applicable.

Consent for publication

Not applicable.

References

1. Kenny HC, Abel ED. Heart Failure in Type 2 Diabetes Mellitus[J]. Circ Res. 2019;124(1):121–41. DOI:10.1161/circresaha.118.311371.
2. Dunlay SM, Roger VL, Redfield MM. Epidemiology of heart failure with preserved ejection fraction[J]. Nat Rev Cardiol. 2017;14(10):591–602. DOI:10.1038/nrcardio.2017.65.
3. Athithan L, Gulsin GS, McCann GP, et al. Diabetic cardiomyopathy: Pathophysiology, theories and evidence to date[J]. World J Diabetes. 2019;10(10):490–510. DOI:10.4239/wjd.v10.i10.490.
4. Mátyás C, Kovács A, Németh BT, et al. Comparison of speckle-tracking echocardiography with invasive hemodynamics for the detection of characteristic cardiac dysfunction in type-1 and type-2 diabetic rat models[J]. Cardiovasc Diabetol. 2018;17(1):13. DOI:10.1186/s12933-017-0645-0.
5. Chareonthaitawee P, Sorajja P, Rajagopalan N, et al. Prevalence and prognosis of left ventricular systolic dysfunction in asymptomatic diabetic patients without known coronary artery disease referred for stress single-photon emission computed tomography and assessment of left ventricular function[J]. Am Heart J. 2007;154(3):567–74. DOI:10.1016/j.ahj.2007.04.042.
6. Singh RM, Waqar T, Howarth FC, et al. Hyperglycemia-induced cardiac contractile dysfunction in the diabetic heart[J]. Heart Fail Rev. 2018;23(1):37–54. DOI:10.1007/s10741-017-9663-y.
7. O'Brien T, Nguyen TT, Zimmerman BR. Hyperlipidemia and diabetes mellitus[J]. Mayo Clin Proc. 1998;73(10):969–76. DOI:10.4065/73.10.969.
8. Yamagishi S. Cardiovascular disease in recent onset diabetes mellitus[J]. J Cardiol. 2011;57(3):257–62. DOI:10.1016/j.jjcc.2011.01.011.
9. Sun M, Sun L, Huang C, et al. Induction of Macrophage M2b/c Polarization by Adipose Tissue-Derived Mesenchymal Stem Cells[J]. J Immunol Res, 2019, 2019(7059680. DOI:10.1155/2019/7059680.
10. Zhang S, Picard MH, Vasile E, et al. Diet-induced occlusive coronary atherosclerosis, myocardial infarction, cardiac dysfunction, and premature death in scavenger receptor class B type I-deficient, hypomorphic apolipoprotein ER61 mice[J]. Circulation. 2005;111(25):3457–64. DOI:10.1161/circulationaha.104.523563.
11. Minguell JJ, Erices A. Mesenchymal stem cells and the treatment of cardiac disease[J]. Exp Biol Med (Maywood). 2006;231(1):39–49.
12. White SJ, Chong JJH. Mesenchymal Stem Cells in Cardiac Repair: Effects on Myocytes, Vasculature, and Fibroblasts[J]. Clin Ther. 2020;42(10):1880–91. DOI:10.1016/j.clinthera.2020.08.010.
13. Zou L, Ma X, Lin S, et al. Bone marrow mesenchymal stem cell-derived exosomes protect against myocardial infarction by promoting autophagy[J]. Exp Ther Med. 2019;18(4):2574–82. DOI:10.3892/etm.2019.7874.
14. Liu L, Jin X, Hu CF, et al. Exosomes Derived from Mesenchymal Stem Cells Rescue Myocardial Ischaemia/Reperfusion Injury by Inducing Cardiomyocyte Autophagy Via AMPK and Akt Pathways[J]. Cell Physiol Biochem. 2017;43(1):52–68. DOI:10.1159/000480317.

15. Maharlooei MK, Bagheri M, Solhjou Z, et al. Adipose tissue derived mesenchymal stem cell (AD-MSC) promotes skin wound healing in diabetic rats[J]. Diabetes Res Clin Pract. 2011;93(2):228–34. DOI:10.1016/j.diabres.2011.04.018.
16. Yin Q, Xu N, Xu D, et al. Comparison of senescence-related changes between three- and two-dimensional cultured adipose-derived mesenchymal stem cells[J]. Stem Cell Res Ther. 2020;11(1):226. DOI:10.1186/s13287-020-01744-1.
17. Hu C, Zhao L, Li L. Current understanding of adipose-derived mesenchymal stem cell-based therapies in liver diseases[J]. Stem Cell Res Ther. 2019;10(1):199. DOI:10.1186/s13287-019-1310-1.
18. Xu S, Zhou Z, Li H, et al. BMSCs ameliorate septic coagulopathy by suppressing inflammation in cecal ligation and puncture-induced sepsis[J]. J Cell Sci, 2018, 131(3): DOI:10.1242/jcs.211151.
19. Liang H, Ding X, Yu Y, et al. Adipose-derived mesenchymal stem cells ameliorate acute liver injury in rat model of CLP induced-sepsis via sTNFR1[J]. Exp Cell Res. 2019;383(1):111465. DOI:10.1016/j.yexcr.2019.06.010.
20. Heo J, Choi Y, Kim HJS. c i. Adipose-Derived Mesenchymal Stem Cells Promote M2 Macrophage Phenotype through Exosomes[J]. 2019, 2019(7921760. DOI: 10.1155/2019/7921760.
21. Sun M, Sun L, Huang C, et al. Induction of Macrophage M2b/c Polarization by Adipose Tissue-Derived Mesenchymal Stem Cells[J]. 2019, 2019(7059680. DOI: 10.1155/2019/7059680.
22. Peet C, Ivetic A, Bromage DI, et al. Cardiac monocytes and macrophages after myocardial infarction[J]. Cardiovasc Res. 2020;116(6):1101–12. DOI:10.1093/cvr/cvz336.
23. Shah SJ, Kitzman DW, Borlaug BA, et al. Phenotype-Specific Treatment of Heart Failure With Preserved Ejection Fraction: A Multiorgan Roadmap[J]. Circulation. 2016;134(1):73–90. DOI:10.1161/circulationaha.116.021884.
24. Sano S, Oshima K, Wang Y, et al. Tet2-Mediated Clonal Hematopoiesis Accelerates Heart Failure Through a Mechanism Involving the IL-1β/NLRP3 Inflammasome[J]. J Am Coll Cardiol. 2018;71(8):875–86. DOI:10.1016/j.jacc.2017.12.037.
25. Everett BM, Cornel JH, Lainscak M, et al. Anti-Inflammatory Therapy With Canakinumab for the Prevention of Hospitalization for Heart Failure[J]. Circulation. 2019;139(10):1289–99. DOI:10.1161/circulationaha.118.038010.
26. Xiang E, Han B, Zhang Q, et al. Human umbilical cord-derived mesenchymal stem cells prevent the progression of early diabetic nephropathy through inhibiting inflammation and fibrosis[J]. Stem Cell Res Ther. 2020;11(1):336. DOI:10.1186/s13287-020-01852-y.
27. Dai R, Liu J, Cai S, et al. Delivery of adipose-derived mesenchymal stem cells attenuates airway responsiveness and inflammation in a mouse model of ovalbumin-induced asthma[J]. Am J Transl Res. 2017;9(5):2421–8.
28. Hamada D, Maynard R, Schott E, et al. Suppressive Effects of Insulin on Tumor Necrosis Factor-Dependent Early Osteoarthritic Changes Associated With Obesity and Type 2 Diabetes Mellitus[J]. 2016, 68(6): 1392–1402. DOI: 10.1002/art.39561.

29. Dei Cas A, Khan S, Butler J, et al. Impact of diabetes on epidemiology, treatment, and outcomes of patients with heart failure[J]. 2015, 3(2): 136–145. DOI: 10.1016/j.jchf.2014.08.004.
30. Rios FJ, Touyz RM, Montezano AC. Isolation and Differentiation of Murine Macrophages[J]. Methods Mol Biol. 2017;1527:297–309. DOI:10.1007/978-1-4939-6625-7_23.
31. Emile JF, Abla O, Fraitag S, et al. Revised classification of histiocytoses and neoplasms of the macrophage-dendritic cell lineages[J]. Blood. 2016;127(22):2672–81. DOI:10.1182/blood-2016-01-690636.
32. Hahn O, Ingwersen LC, Soliman A, et al. TGF-ß1 Induces Changes in the Energy Metabolism of White Adipose Tissue-Derived Human Adult Mesenchymal Stem/Stromal Cells In Vitro[J]. Metabolites, 2020, 10(2): DOI:10.3390/metabo10020059.
33. Shree N, Venkategowda S, Venkatranganna M, et al. Human adipose tissue mesenchymal stem cells as a novel treatment modality for correcting obesity induced metabolic dysregulation[J]. 2019, 43(10): 2107–2118. DOI: 10.1038/s41366-019-0438-5.
34. He C, Bassik MC, Moresi V, et al. Exercise-induced BCL2-regulated autophagy is required for muscle glucose homeostasis[J]. Nature. 2012;481(7382):511–5. DOI:10.1038/nature10758.
35. Lee IH, Kawai Y, Fergusson MM, et al. Atg7 modulates p53 activity to regulate cell cycle and survival during metabolic stress[J]. Science. 2012;336(6078):225–8. DOI:10.1126/science.1218395.
36. Weindel CG, Richey LJ, Bolland S, et al. B cell autophagy mediates TLR7-dependent autoimmunity and inflammation[J]. Autophagy. 2015;11(7):1010–24. DOI:10.1080/15548627.2015.1052206.
37. Ju L, Han J, Zhang X, et al. Obesity-associated inflammation triggers an autophagy-lysosomal response in adipocytes and causes degradation of perilipin 1[J]. Cell Death Dis. 2019;10(2):121. DOI:10.1038/s41419-019-1393-8.
38. Muriach M, Flores-Bellver M, Romero FJ, et al. Diabetes and the brain: oxidative stress, inflammation, and autophagy[J]. Oxid Med Cell Longev, 2014, 2014(102158. DOI:10.1155/2014/102158.
39. Kolattukudy PE, Niu J. Inflammation, endoplasmic reticulum stress, autophagy, and the monocyte chemoattractant protein-1/CCR2 pathway[J]. Circ Res. 2012;110(1):174–89. DOI:10.1161/circresaha.111.243212.

Tables

Tabel 1 Primes Sequence

Gene	Sequence
TNF-α (mouse)	Forward5’CAGGCGGTGCCTATGTCTC3’
	Reverse5’CAGGCGGTGCCTATGTCTC3’
CXCL15 (mouse)	Forward5’TCGAGACCATTTACTGCAACAG3’
	Reverse5’CATTGCCGGTGGAAATTCCTT3’
IL-6 (mouse)	Forward5’ CTGCAAGAGACTTCCATCCAG3’
	Reverse5’AGTGGTATAGACAGGTCTGTTGG3’

Supplementary Tables

Supplemental Table 1 is not available with this version.

Figures

Figure 1

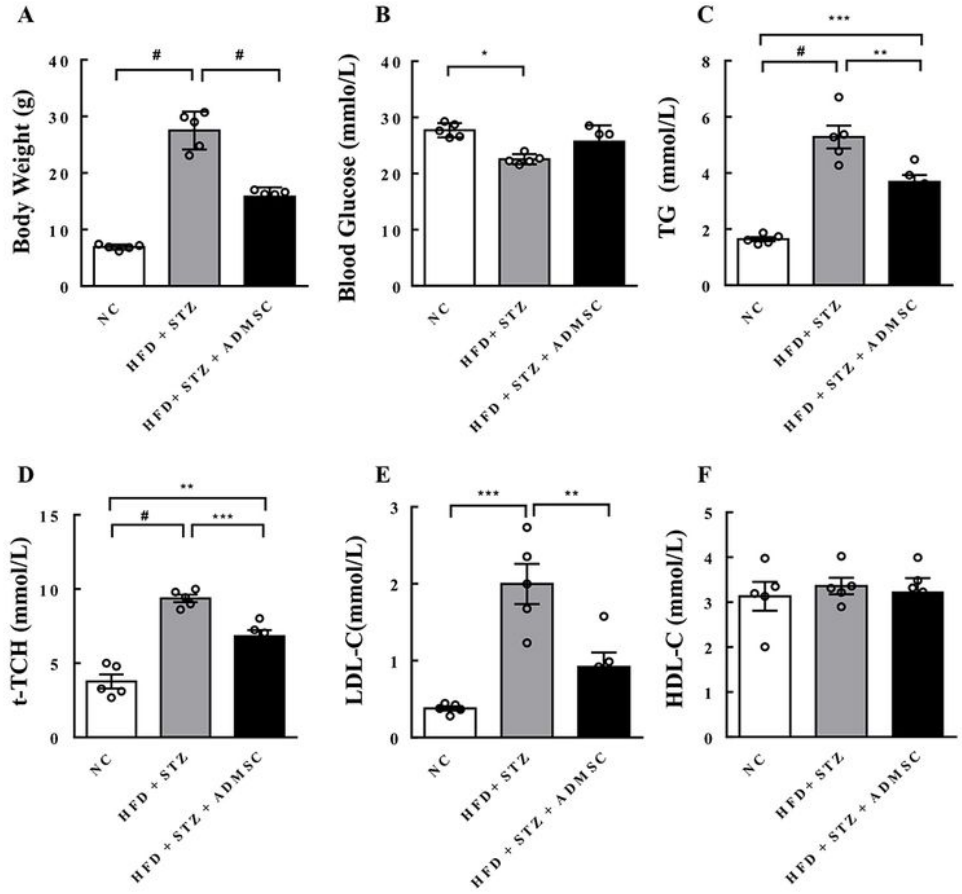

Figure 1

Adipose tissue-derived stem cells（ADSCs）improved glycometabolism and lipid metabolism of high-fat diet/STZ -induced diabetic mice. (A) Body weight (n=6 mice/group). (B) Blood glucose (n=6 mice/group). (C) Serum triglyceride (n=6 mice/group). (D) Total cholesterol (n=6 mice/group). (E) low-density lipoprotein cholesterol (n=6 mice/group) (F) High-density lipoprotein cholesterol (n=6 mice/group). NC, wild type mice with normal chaw; HFD+STZ mice, high-fat diet/STZ-induced diabetic;

HFD+STZ+ADMSCs mice, high-fat diet/STZ-induced diabetic mice injected with ADMSCs. Data are mean±SEM, One-way ANOVA with Bonferroni post-test, *P<0.05, **P<0.01, ***P<0.005, #P<0.0001.

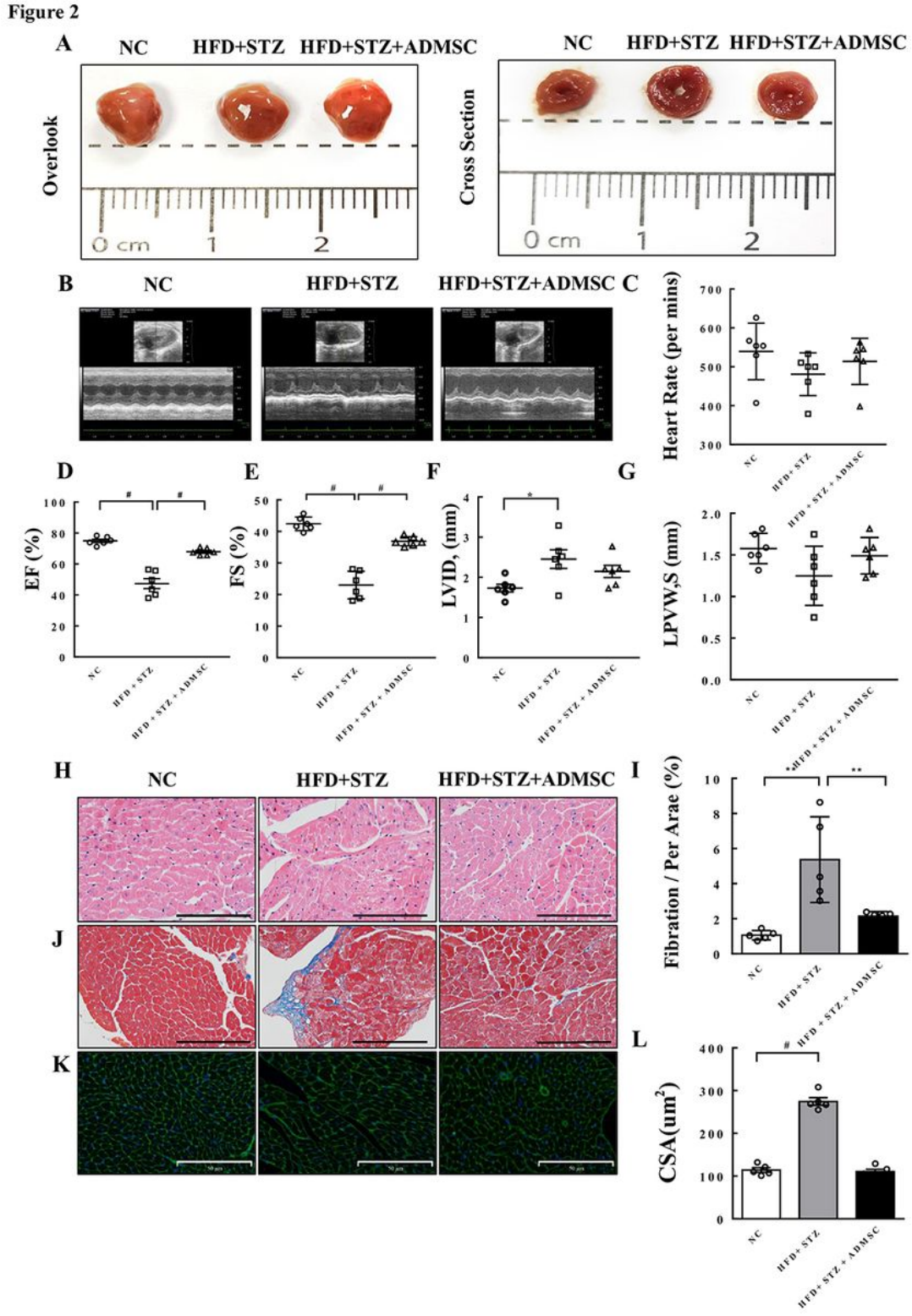

Figure 2

Adipose tissue-derived stem cells（ADMSCs）alleviated heart failure of high-fat diet/STZ -induced diabetic mice. (A) The overlook of hearts. (B) Representative M-mode traces from left ventricular short axis view (n=6 mice/group) (C) Heart rates (n=6 mice/group) (D) Ejection fraction (n=6 mice/group) (E) Left

ventricular short-axis shortening rate (n=6 mice/group) (F) Left ventricular internal dimension (n=6 mice/group) (G) End diastolic of the posterior wall of the left ventricle (n=6 mice/group) (H) HE staining of heart tissue (n=4 scopes/group). Scar bar, 50 μm.(I) Masson staining of heart tissue (n=5 scopes/group). Scar bar, 50 μm (J)WGA staining of myocardial cells(n=5 scopes/group). Scar bar, 50 μm (K) and (L) Representative quantification of (J) and (L). WT, wild type mice with normal diet; HFD+STZ mice, high-fat diet/STZ-induced diabetic; HFD+STZ+ADSCs mice, high-fat diet/STZ-induced diabetic mice injected with ADSCs. Data are mean±SEM, One-way ANOVA with Bonferroni post-test, *P<0.05, **P<0.01, ***P<0.005, #P<0.0001.

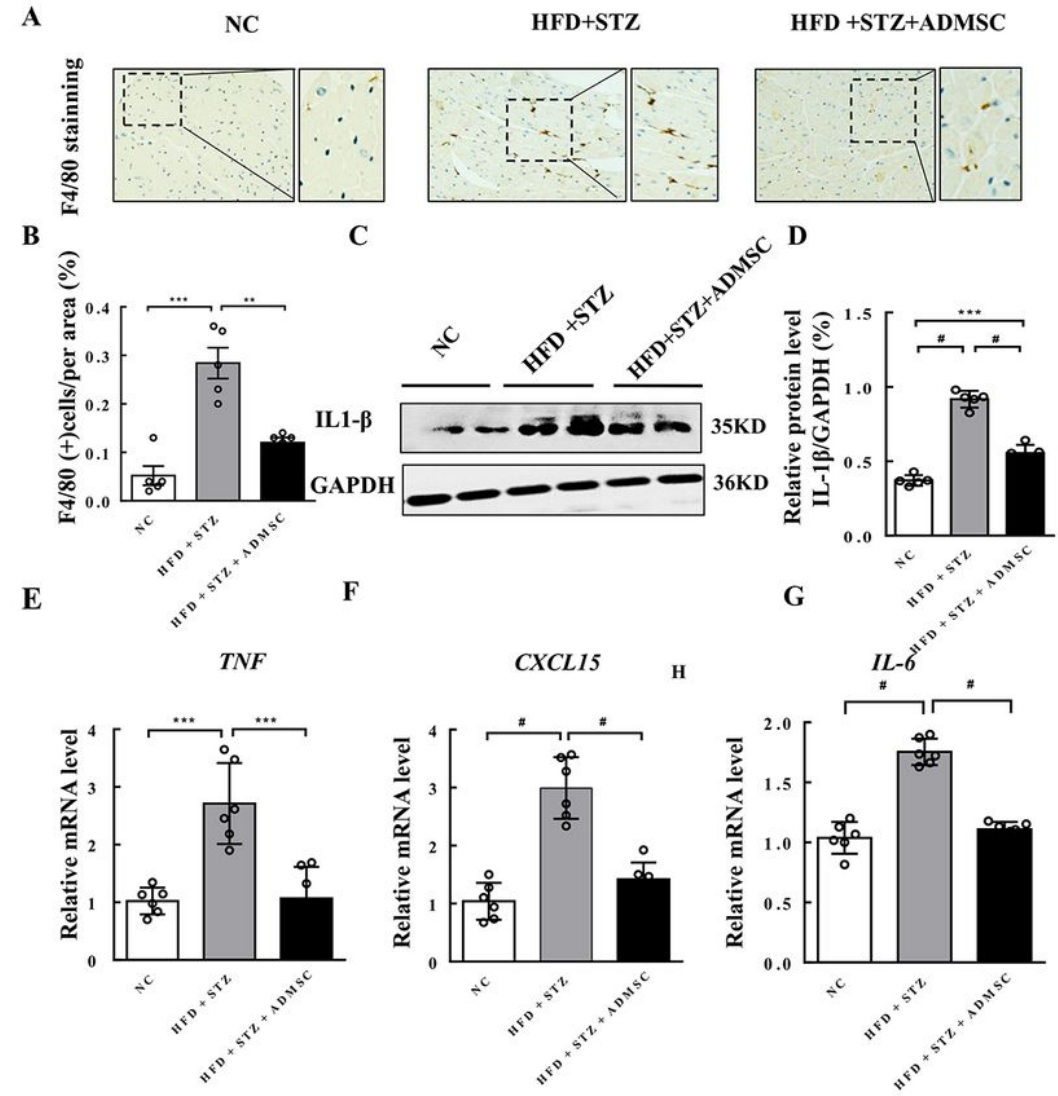

Figure 3

Adipose tissue-derived stem cells（ADMSCs）promoted adhesion of macrophages and the secretion of IL-1β in vivo and in vitro. (A) IHC staining of F4/80 in cardiac tissue (n=5 mice/group, 4 scopes/mice,). Scar bar, 100 μm. (B) Quantification of (A). (C) The expression of IL-1β in mice of three groups. The protein level was detected by western blot analysis (n=5/group). (D) Quantification of (C). (E) The mRNA level of TNFα, CXCL15 and IL-6 in cardiac tissue of three groups (n=5 mice/group). (F) Schematic diagram for the

co-culture system of ADMSCs and macrophages. NC, wild type mice with normal diet; HFD+STZ mice, high-fat diet/STZ-induced diabetic; HFD+STZ+ADMSCs mice, high-fat diet/STZ-induced diabetic mice injected with ADMSCs. TNFα, tumor necrosis factor α; IL-8, interleukin 8; IL-6, interleukin 6; HG, high glucose. Data are mean±SEM, One-way ANOVA with Bonferroni post-test, *P<0.05, **P<0.01, ***P<0.005, #P<0.0001.

Figure 4

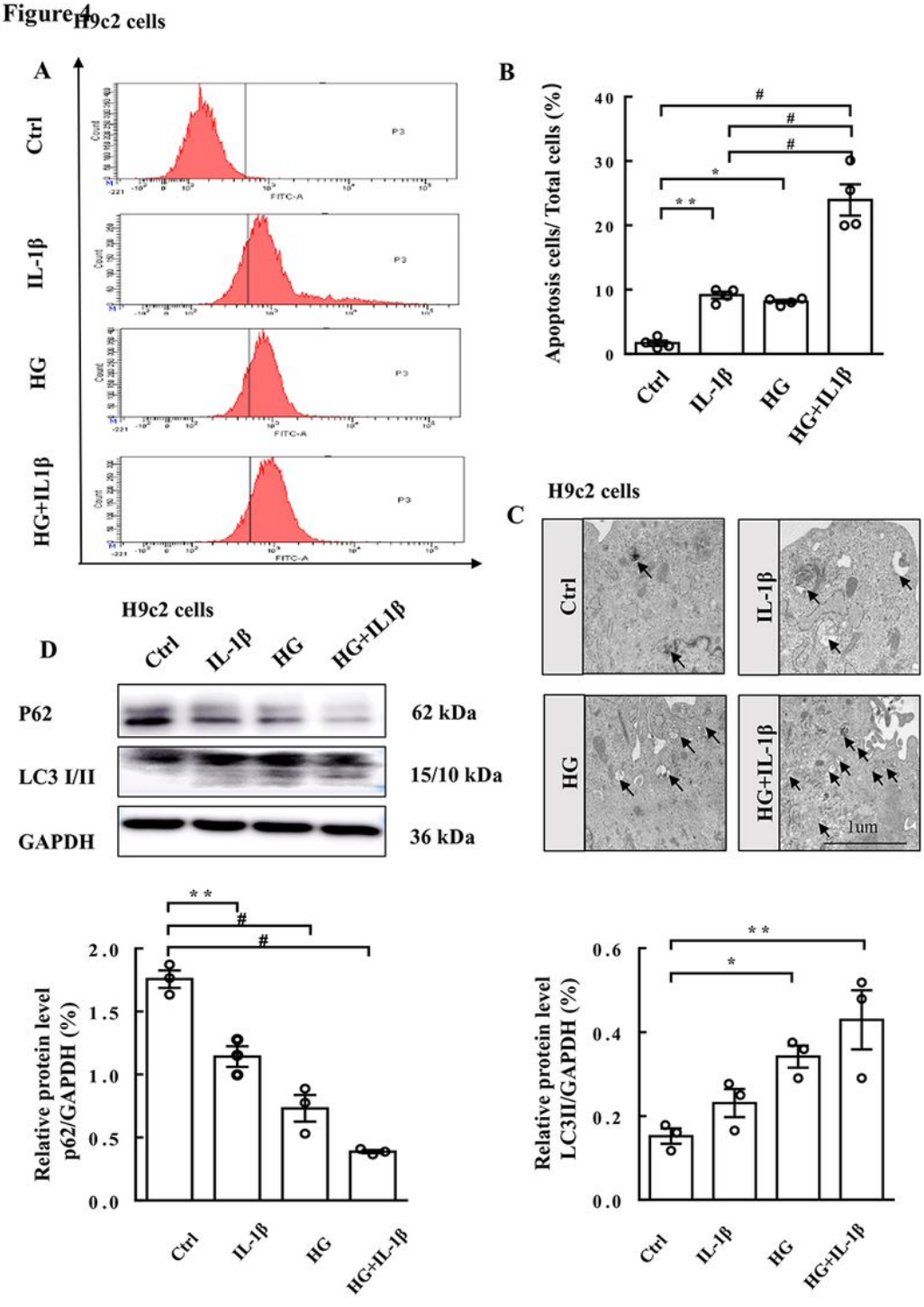

IL-1β enhanced diabetic cardiomyopathy by inhibiting autophagy and increasing apoptosis in H9c2 cells. (A) Apoptosis of H9c2 were measured by flow cytometry. (B) Quantification of (A). (C)The transmission electron microscope of autophagic vacuolization was decreased in IL-1β and HG stimulated H9c2 (magnification, ×5000, ×15,000). (D) The protein level of LC3I/II, P62 and Beclin1 in control and treated groups (n=4/group). (E) Quantification of (D). Data are mean±SEM, One-way ANOVA with Bonferroni post-test, *P<0.05, **P<0.01, ***P<0.005, #P<0.0001.

Figure 5

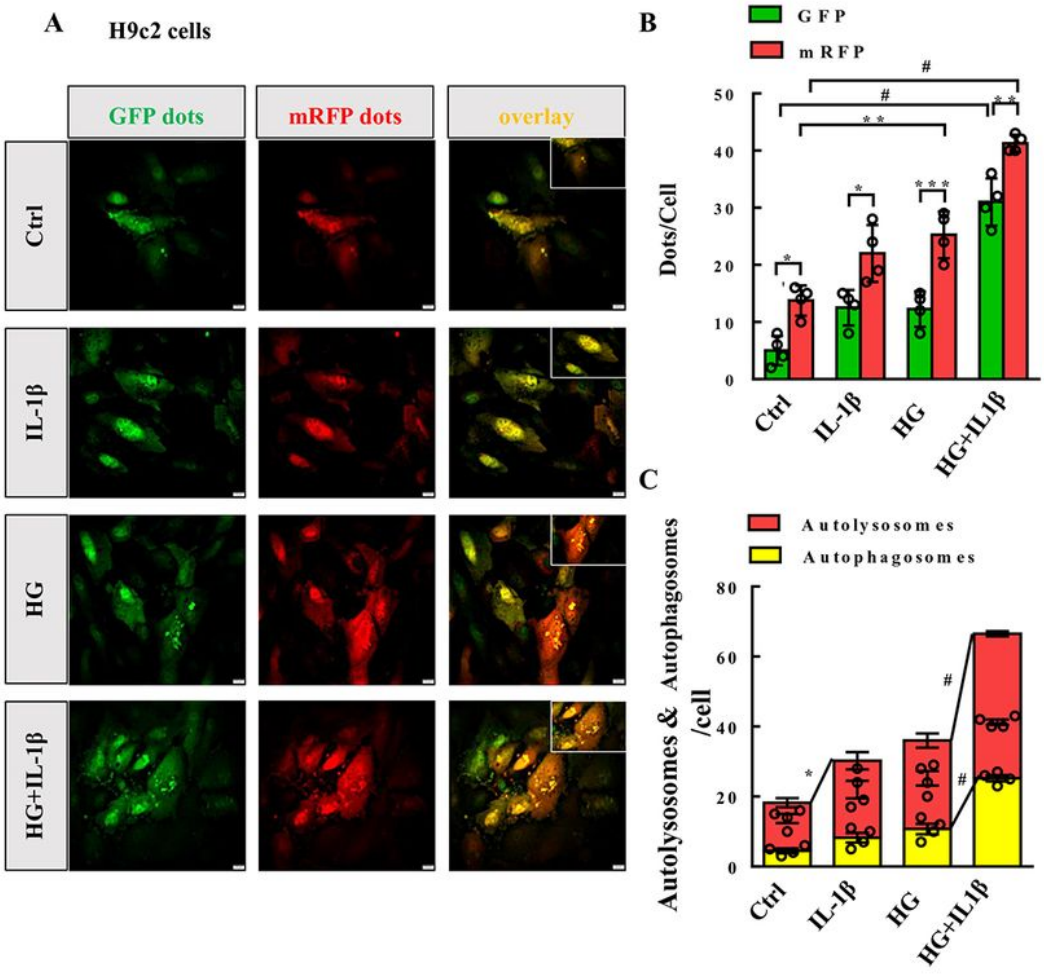

Figure 5

(A) Autophagosomes and autolysosomes were detected by tandem fluorescent mRFG-GFP-LC3 assay (n=4 scopes/group). Yellow foci represent autophagosomes (GFP and mRFP overlayed), red foci represent autolysosome. Scar Bar, 10 μm. (B)&(C) Quantification of (A). Data are mean±SEM, two-way ANOVA with Bonferroni post-test, *P<0.05, **P<0.01, ***P<0.005, #P<0.0001.